Data-Driven Approach to Discovery of Physical Mechanisms in Biomechanical Systems

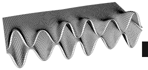

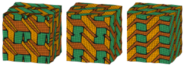

Siddhartha Srivastava Zhenlin Wang Denislav Nikolov Bachir Abeid Ulrich Scheven Ellen Arruda Johannes Weickenmeier Jon Estrada Krishna Garikipati

Departments of Mechanical Engineering and Mathematics
Michigan Institute for Computational Discovery & Engineering
University of Michigan, Ann Arbor

Society of Engineering Science Annual Technical Meeting, 2022

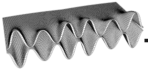

Data-Driven approaches

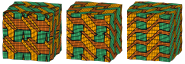

- Physical System $\Longrightarrow$ Data $\Longrightarrow$ Governing Equation
- The exact form of governing equation may not be known.

Physical System:

Solid mechanics

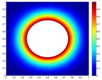

Heat flow

Strong form:

$$\nabla \cdot \left(\mathbb{C} : \nabla^{\mathrm{s}} \boldsymbol{u}^{\mathrm{d}}\right) \approx 0$$

$$\frac{\partial \theta^{\mathrm{d}}}{\partial t} \approx \nabla \cdot \left(\kappa \nabla \theta^{\mathrm{d}}\right)$$

Weak form:

$$\int_\Omega \nabla^{\mathrm{s}} \boldsymbol{w} : \mathbb{C} : \nabla^{\mathrm{s}} \boldsymbol{u}^{\mathrm{d}} d\Omega \approx \int_{\partial\Omega} \boldsymbol{w} \cdot \boldsymbol{T} dS$$

$$\int_\Omega \left(\frac{\partial \theta^{\mathrm{d}}}{\partial t} w + \kappa \nabla \theta^{\mathrm{d}} \cdot \nabla w\right) d\Omega \approx \int_{\partial\Omega} j_n w dS$$

- Choice of basis functions allows continuous representations from possibly discrete data with desired regularity
- Boundary conditions appear naturally in the weak form.

- Different mechanisms of deformation are encoded in constitutive relationships of these materials.
- Many tissues and ligaments admit to hyperelastic models.
- Muscle fibers may introduce anisotropy.
- Growth in biomechanical systems like the brain admits to Morphoelastic models.
- Many other mechanisms to choose from, e.g., viscoelasticity, damage models, inelasticity etc.

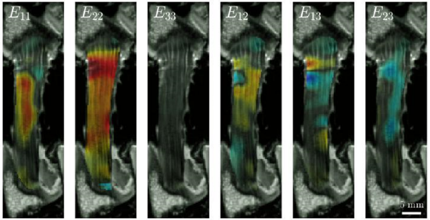

Deformation of ACL (anterior cruciate ligament)

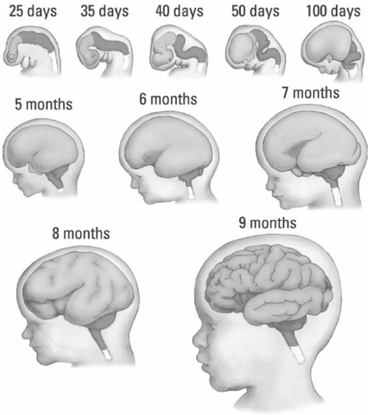

Brain growth

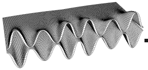

Discovery of constitutive models of soft materials

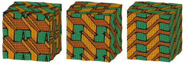

- Collect data of displacement fields for a soft elastomer

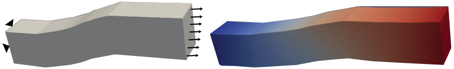

- Find parameter fits for a single chosen model (Neo-Hookean strain energy density function):

$$W(\boldsymbol{C}) = \frac{1}{2}\kappa(J-1)^2 + \frac{1}{2}\mu(\bar{I}_1 - 3)$$

- We want to discover the proper physics from a large range of *possible* mechanism.

$$W(\boldsymbol{C}) = \underbrace{\frac{1}{2}\kappa(J-1)^2}_{\text{volumetric}} + \underbrace{\frac{1}{2}\mu(\bar{I}_1 - 3) + \theta_1(\bar{I}_1 - 3)^2 + \theta_2(\bar{I}_2 - 3) + \theta_3(\bar{I}_2 - 3)^2}_{\text{isochoric}} + \underbrace{\theta_4(\bar{I}_a - 1) + \theta_5(\bar{I}_a - 1)^2}_{\text{orthotropic}}$$
$$+ \underbrace{\theta_6\left(\exp(\theta_7\left[(\theta_8\bar{I}_1 + (1-3\theta_a)\bar{I}_a - 1)^2\right]\right)}_{\text{HGO model: fiber dispersion}} + \ldots$$

- Infer a parsimonious representation

Z. Wang, J.B. Estrada, E.M. Arruda, K. Garikipati, 2020, submitted to *JMPS*

Outline of the talk

Methods for infering constitutive relations:

- Variational System Identification
- PDE-Constrained optimization

Applications:

- Deformation mechanism identification in Ligament
- Parameter estimation in Ogden hyperelastic model
- Morphoelastic models for Brain growth

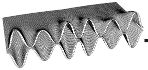

Variational System Identification approach

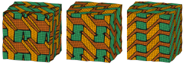

- Start with a large basis for the ansatz for strain energy function:

$$W(\boldsymbol{C}) = \underbrace{\frac{1}{2}\kappa(J-1)^2}_{\text{volumetric}} + \underbrace{\frac{1}{2}\mu(\bar{I}_1-3) + \theta_1(\bar{I}_1-3)^2 + \theta_2(\bar{I}_2-3) + \theta_3(\bar{I}_2-3)^2}_{\text{isochoric}} + \underbrace{\theta_4(\bar{I}_a-1) + \theta_5(\bar{I}_a-1)^2}_{\text{orthotropic}} + \cdots$$

- The first Piola-Kirchhoff stress tensor is $\boldsymbol{P} = \partial W/\partial \boldsymbol{F}$:

$$\boldsymbol{P} = \kappa \boldsymbol{P}_0(J,\boldsymbol{F}) + \mu \boldsymbol{P}_{\mathrm{s}}(\bar{I}_1,\boldsymbol{F}) + \theta_1 \boldsymbol{P}_1(\bar{I}_1,\boldsymbol{F}) + \theta_2 \boldsymbol{P}_2(\bar{I}_2,\boldsymbol{F}) + \theta_3 \boldsymbol{P}_3(\bar{I}_2,\boldsymbol{F}) + \theta_4 \boldsymbol{P}_4(\bar{I}_a,\boldsymbol{F}) + \ldots$$

- Weak form of the stress equilibrium equation:

$$\int_\Omega \frac{\partial \boldsymbol{w}}{\partial \boldsymbol{X}} : \left(\kappa \boldsymbol{P}_0 + \mu \boldsymbol{P}_{\mathrm{s}} + \theta_1 \boldsymbol{P}_1 \ldots\right) \mathrm{d}V - \int_{\Gamma_T} \boldsymbol{w} \cdot \boldsymbol{T} \mathrm{d}S = \boldsymbol{0}$$

- Residual vector is assembled:

$$\boldsymbol{R} = -\sum_e \left[\int_{\Omega_e} \nabla \boldsymbol{N} \cdot \left(\kappa \boldsymbol{P}_0^{\mathrm{d}} + \mu \boldsymbol{P}_{\mathrm{s}}^{\mathrm{d}} + \theta_1 \boldsymbol{P}_1^{\mathrm{d}} \ldots\right) \mathrm{d}V - \int_{\Gamma_{T_e}} \boldsymbol{N} \otimes \boldsymbol{T} \mathrm{d}S\right]$$

- The coefficients can be found by minimizing $\boldsymbol{R}^2$

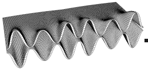

Operator elimination for parsimonious model

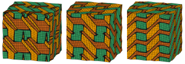

- A parsimonious model is obtained by dropping less relevant operators.
- Each node of the graph represents a selection of operator with more operators on top nodes and fewer operators on the bottom nodes.
- Operator elimination is synonymous to traversing downwards on the graph. Methods include Stepwise regression (greedy algorithm), Genetic Algorithm, Monte Carlo tree search.

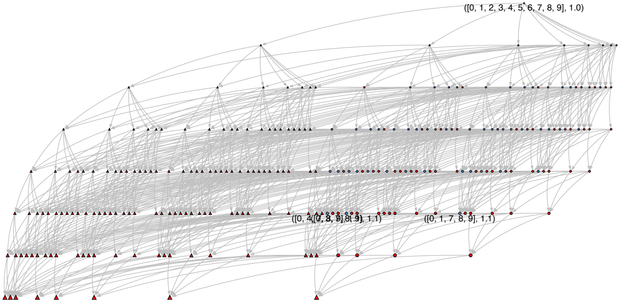

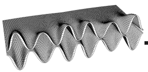

Operator elimination for parsimonious model: Stepwise Regression

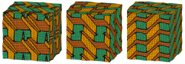

- Parsimonious model is obtained by dropping operators based on F-Test

$$F = \frac{\text{Loss}\,(\boldsymbol{\theta}|\theta_i = 0) - \text{Loss}\,(\boldsymbol{\theta})}{\text{Loss}\,(\boldsymbol{\theta})} \times \#\ \text{Dropped Parameters}$$

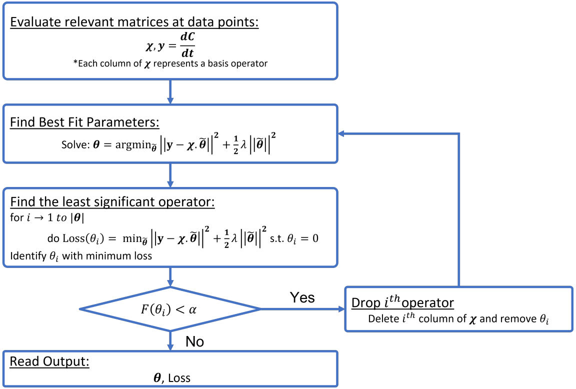

- Drop the operator corresponding to θ_i, if F is less than a threshold value.
- Repeat the step multiple times at each time step to reduce number of operators.

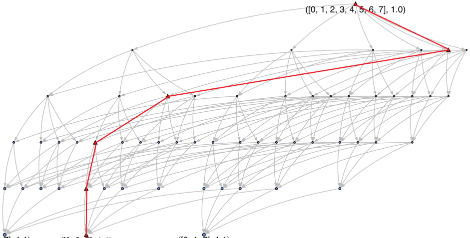

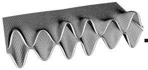

Discovery of constitutive models of soft materials

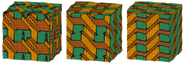

True model: $\kappa = 8000$ kPa and $\mu = 80$ kPa

Data origin	Noise (σ mm)	κ kPa	μ kPa	θ_1	θ_2 kPa	θ_3 kPa	θ_4 kPa	θ_5 kPa
Extension 1	0	7616	80.2	E	E	E	S	S
	0.0001	7286.8	94.6	E	E	E	S	S
	0.001	40	120	E	E	E	S	S
Extension 2	0	7493.0	83.0	E	E	E	E	E
	0.0001	1406.6	83.4	E	E	E	E	E
	0.001	615.6	112.0	E	E	E	E	E
Bending	0	8000.0	80.0	E	E	E	S	E
	0.0001	10.6	74.8	E	E	E	S	E
	0.001	0.0	31.4	E	E	E	S	E
Torsion	0	5827.8	93.6	E	E	E	E	E
	0.0001	3623.6	97.2	E	E	E	E	E
	0.001	0.0	103.2	E	E	E	E	E
Combined	0	7494.6	83.0	E	E	E	E	E
	0.0001	7200.0	84.8	E	E	E	E	E
	0.001	1985.6	115.6	E	E	E	E	E

- Accurate estimation of mechanisms
- Reasonably good but inconsistent inference of parameters in presence of noise.

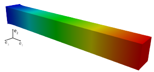

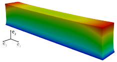

Extension 1, along $\boldsymbol{e}_1$ Extension 2, along $\boldsymbol{e}_2$

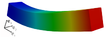

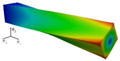

Bending Torsion

The four boundary value problems for generation of synthetic data.

Z Wang, J.B. Estrada, E.M. Arruda, K. Garikipati *JMPS*, 2021

PDE Constrained Optimization for Model refinement

- Variational System Identification technique offers a fast and robust approach for mechanism identification, however, the parameters may not be accurate. This problem is exacerbated in following sitation.
  - near-incompressibility of the response ($J \sim 1$)
  - large noise in the experimental data
  - choice of proper spatial filter
- PDE constrained Optimization estimate parameters that minimizes the difference between the data and forward solution of the PDE.
- Minimize following cost function:

$$\text{Cost}(\kappa, \mu, \theta_1, \cdots) = \int_\Omega |\boldsymbol{u}^{\text{FE}} - \boldsymbol{u}^{\text{data}}| d\Omega$$

$$\textbf{subject to } \boldsymbol{R}(\boldsymbol{u}^{FE}; \kappa, \mu, \theta_1, \cdots) = \mathbf{0}$$

- Adjoint based optimization is used for estimating gradients. Software Package: `fenics`, `dolfin-adjoint`

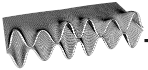

Discovery of constitutive models of soft materials

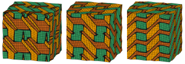

True model: $W = 4000(J-1)^2 + 40(\bar{I}_1 - 3)$ kJm^{-3}

Data origin	Noise (σ mm)	Identified strain energy density function (kJm^{-3})
Extension 1	0	$W = 4000.00(J-1)^2 + 40.00(\bar{I}_1 - 3)$
	0.0001	$W = 3999.99(J-1)^2 + 40.00(\bar{I}_1 - 3)$
	0.001	$W = 4000.13(J-1)^2 + 40.00(\bar{I}_1 - 3)$
Extension 2	0	$W = 4000.02(J-1)^2 + 40.00(\bar{I}_1 - 3)$
	0.0001	$W = 4000.02(J-1)^2 + 40.00(\bar{I}_1 - 3)$
	0.001	$W = 3998.80(J-1)^2 + 40.00(\bar{I}_1 - 3)$
Bending	0	$W = 4000.00(J-1)^2 + 40.00(\bar{I}_1 - 3)$
	0.0001	$W = 4099.36(J-1)^2 + 39.46(\bar{I}_1 - 3)$
	0.001	$W = 3999.99(J-1)^2 + 40.00(\bar{I}_1 - 3)$
Torsion	0	$W = 4000.00(J-1)^2 + 40.00(\bar{I}_1 - 3)$
	0.0001	$W = 3999.74(J-1)^2 + 40.00(\bar{I}_1 - 3)$
	0.001	$W = 3979.70(J-1)^2 + 40.00(\bar{I}_1 - 3)$

- Accurate inference of parameters even in presence of noise.

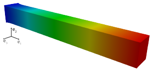

Extension 1, along $\boldsymbol{e}_1$

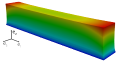

Extension 2, along $\boldsymbol{e}_2$

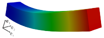

Bending

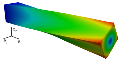

Torsion

The four boundary value problems for generation of synthetic data.

Z Wang, J.B. Estrada, E.M. Arruda, K. Garikipati *JMPS*, 2021

Soft and bio-materials (such as anterior cruciate ligament) have a variety of complicated material behavior. In many cases, the choice of material model is not firmly established.

- Full-field displacement capture (FFDC) via MR-**u**
  - entire displacement and deformation tensor field
  - spatial filter is needed on the experimental data

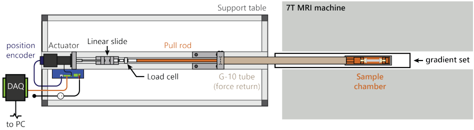

We aim to:

- discover the proper physics from a large range of possible mechanism
- quantify the uncertainty in the identified mechanism.

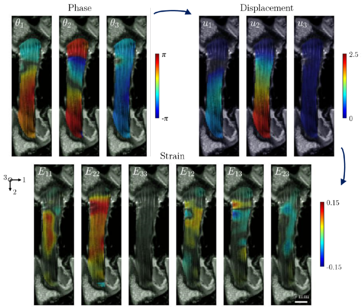

Full-field displacement capture (FFDC) via MR-**u** of an Anterior Cruciate Ligament (ACL tissue)

J. Estrada, U. Scheven, C. Luetkemeyer, and E. Arruda, *Experimental Mechanics*, 2020

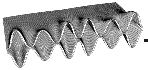

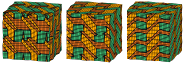

- Ansatz for strain energy

$$W(\boldsymbol{C}) = \underbrace{\frac{1}{2}\kappa(J-1)^2}_{\text{volumetric}} + \underbrace{\frac{1}{2}\mu(\bar{I}_1 - 3) + \theta_1(\bar{I}_1 - 3)^2 + \theta_2(\bar{I}_2 - 3) + \theta_3(\bar{I}_2 - 3)^2}_{\text{isochoric}} + \underbrace{\theta_4(\bar{I}_a - 1) + \theta_5(\bar{I}_a - 1)^2}_{\text{orthotropic}}$$

$$+ \underbrace{\theta_6 \left(\exp(\theta_7 \left[(\theta_8 \bar{I}_1 + (1 - 3\theta_a)\bar{I}_a - 1)^2 \right] \right)}_{\text{HGO model: fiber dispersion}} + \ldots$$

- Inferred form:

$$W(\boldsymbol{C}) = \underbrace{37(J-1)^2}_{\text{volumetric}} + \underbrace{0.52(\bar{I}_1 - 3)}_{\text{isochoric}}$$

$$+ \underbrace{44.2 \left(\exp(\left[(3.2\bar{I}_1 + 0.7\bar{I}_a - 1)^2 \right] \right)}_{\text{HGO model: fiber dispersion}}$$

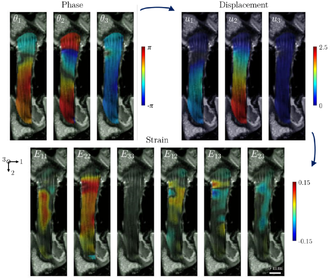

Full-field displacement capture (FFDC) via MR-**u** of an Anterior Cruciate Ligament (ACL tissue)

Z Wang, J.B. Estrada, E.M. Arruda, K. Garikipati *JMPS*, 2021

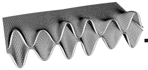

Discovery of constitutive models of soft materials

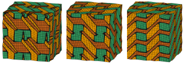

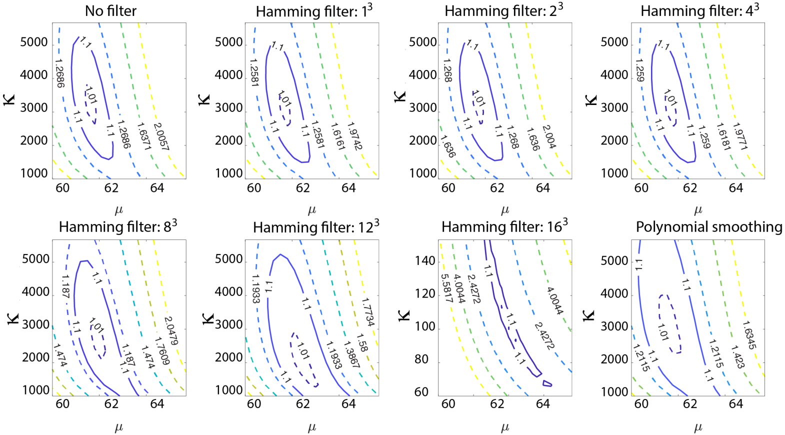

This ratio for the solid curves is $\frac{\text{error}_{\text{solid}}}{\text{error}_{\text{min}}} = 1.1$.

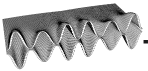

Phenomenological models - Ogden model

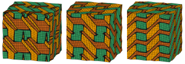

A popular hyperelasticity model with a Helmholtz free energy per reference volume that is expressed in terms of the applied principal stretches.

$$\Psi = \frac{\kappa}{2}(\ln J)^2 + \sum_{i=1}^{N} \frac{\mu_i}{\alpha_i}\left(\overline{\lambda}^{\alpha_i} + \overline{\lambda}^{\alpha_i} + \overline{\lambda}^{\alpha_i} - 3\right).$$

where $\overline{\lambda}_i = J^{-1/3}\lambda_i$ represent the isochoric versions of the principal stretches. The first Piola-Kirchhoff stress $\boldsymbol{P} = d\Psi(\boldsymbol{F})/d\boldsymbol{F}$ is then

$$\boldsymbol{P} = \left(\sum_{j=1}^{3} \tau_j \boldsymbol{n}^j \otimes \boldsymbol{n}^j\right) \boldsymbol{F}^{-T},$$

$$\text{where } \tau_j = \sum_{i=1}^{N} \mu_i J^{-\alpha_i/3}\left(\lambda_j^{\alpha_i} - \frac{1}{3}\left(\lambda_1^{\alpha_i} + \lambda_2^{\alpha_i} + \lambda_3^{\alpha_i}\right)\right) + \kappa \ln J.$$

Proc. R. Soc. Lond. A. **328**, 567–583 (1972)
Printed in Great Britain

Large deformation isotropic elasticity: on the correlation of theory and experiment for compressible rubberlike solids

By R. W. Ogden
School of Mathematics and Physics, University of East Anglia, Norwich, NOR 88C

(*Communicated by R. Hill, F.R.S. – Received* 17 *January* 1972)

A method of approach to the correlation of theory and experiment for incompressible isotropic elastic solids under finite strain was developed in a previous paper (Ogden 1972). Here, the results of that work are extended to incorporate the effects of compressibility (under isothermal conditions). The strain-energy function constructed for incompressible materials is augmented by a function of the density ratio with the result that experimental data on the compressibility of rubberlike materials are adequately accounted for. At the same time the good fit of the strain-energy function arising in the incompressibility theory to the data in simple tension, pure shear and equibiaxial tension is maintained in the compressible theory without any change in the values of the material constants.
A full discussion of inequalities which may reasonably be imposed upon the material parameters occurring in the compressible theory is included.

- More branches can be added for more complicated stress-strain behaviour (typically 2-3).
- Hill's stability criterion, $\mu_i\alpha_i > 0$ is necessary and sufficient for the strain energy to be admissible.
- A branch doesn't contribute to energy iff $\mu_i \to 0$ or $\alpha_i \to 0$

D.P. Nikolov et al. , *Philosophical Transactions of Royal Society A* (2022)

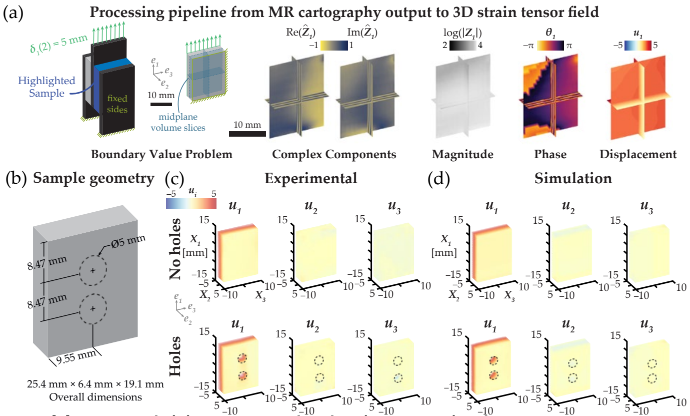

- More spatial heterogeneity in data results in greater information (in the sense of entropy of datasets)

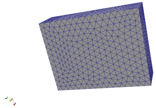

Specimen 1

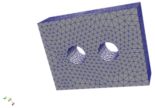

Specimen 2

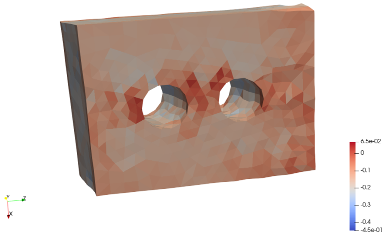

Shear Strain ϵ_{yz}

D.P. Nikolov et al. , *Philosophical Transactions of Royal Society A* (2022)

PDE-constrained optimization procedure:

$$\{\kappa, \alpha_1, \mu_1 \cdots, \alpha_N, \mu_N\} = \underset{\{\widetilde{\kappa}, \widetilde{\alpha_1}, \widetilde{\mu_1} \cdots, \widetilde{\alpha_N}, \widetilde{\mu_N}\}}{\arg\ \min} \{\ell_u + \beta \ell_F\}$$

$$\text{where } \ell_u = \frac{1}{\Omega} \int_\Omega \frac{|\boldsymbol{u}^{\text{FE}} - \boldsymbol{u}|^2}{|\boldsymbol{u}|^2_{max}} \mathrm{d}V \qquad \ell_F = \left(1 - \frac{1}{F_{\text{data}}} \int_{\Gamma_{p^*}} \boldsymbol{p}^* \cdot \boldsymbol{n}\ \mathrm{d}S\right)^2$$

$$\text{subject to: } \boldsymbol{R} = \boldsymbol{0},$$

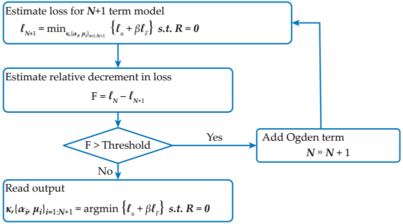

δ_1	κ	μ	$[\mu_1$	$\alpha_1]$	$[\mu_2$	$\alpha_2]$	$[\mu_3$	$\alpha_3]$	ℓ_N $(\times 0.001)$	**F-values**
2.50	2.577e3	16.73	23.08	1.45	-	-	-	-	2.875	
2.50	2.577e3	16.73	23.08	1.45	−0.92	0.00	-	-	2.875	0.000
2.50	2.577e3	16.73	0.00	3.03	23.08	1.45	−0.00	−4.11	2.875	0.000
5.00	2.173e3	16.24	17.00	1.91	-	-	-	-	5.724	
5.00	2.190e3	16.18	17.12	1.89	−4.37	0.00	-	-	5.719	0.005
5.00	2.386e3	16.61	1.23	2.86	17.72	1.65	−0.11	−4.22	5.719	0.000

The values denoted as 0.00 are truncated at two decimal places but represent non-zero values. All moduli are in kPa.

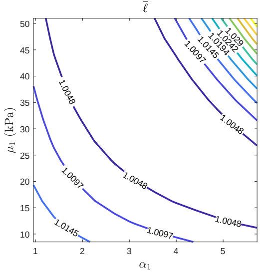

- Consistent prediction of shear modulus, however, material parameters are not consistent between different inference runs.
- The shear modulus (linearized) relates to the material parameter as follows:

$$\mu = \frac{1}{2}\sum_{i=1}^{N} \alpha_i \mu_i$$

- Not enough data that captures the non-linearity in the model.

Morphoelastic growth: Cell positioning drives folding

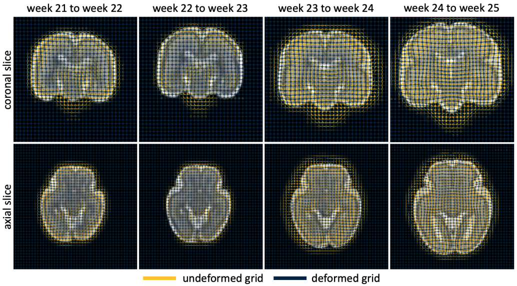

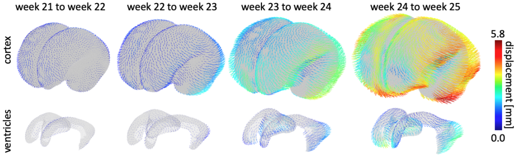

From Verner & KG; 2018

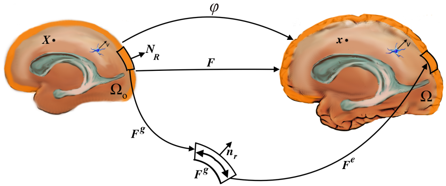

$$\boldsymbol{F} = \boldsymbol{F}^{\mathrm{e}} \boldsymbol{F}^{\mathrm{g}}(c), \qquad c : \text{cell concentration}$$

$$\psi(\boldsymbol{C}^{\mathrm{e}}) = \frac{\lambda}{4}(\det \boldsymbol{C}^{\mathrm{e}} - 1) - \left(\frac{\lambda}{4} + \frac{\mu}{2}\right) \log \det \boldsymbol{C}^{\mathrm{e}} + \frac{\mu}{2}(\mathrm{tr}\, \boldsymbol{C}^{\mathrm{e}} - 3),$$

$$\boldsymbol{P} = \frac{\partial \psi}{\partial \boldsymbol{F}^{e}}, \qquad \nabla \cdot \boldsymbol{P} = \boldsymbol{0} \text{ in } \Omega_0$$

Z Wang et al., *Brain Multiphysics* (2021)

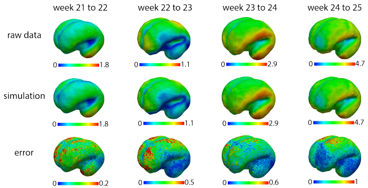

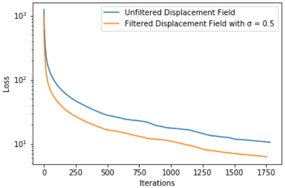

Gaussian Filtering:

$$\widehat{\boldsymbol{u}}(\boldsymbol{x}_0) = \frac{\int_{\mathbb{R}^3} G(\boldsymbol{x}_0, \boldsymbol{x}) \mathrm{d}V}{\int_\Omega G(\boldsymbol{x}_0, \boldsymbol{x}) \mathrm{d}V} \int_\Omega G(\boldsymbol{x}_0, \boldsymbol{x}) \boldsymbol{u}_{\mathrm{reg}}(\boldsymbol{x}) \mathrm{d}V$$

$$= \frac{1}{\int_\Omega G(\boldsymbol{x}_0, \boldsymbol{x}) \mathrm{d}V} \int_\Omega G(\boldsymbol{x}_0, \boldsymbol{x}) \boldsymbol{u}_{\mathrm{reg}}(\boldsymbol{x}) \mathrm{d}V.$$

- Each solution of the adjoint equation is followed by a forward solution for $\boldsymbol{u}_\tau$
- Linearly subdivided χ_τ into 25 steps in driving the forward solution
- Convergence threshold $< 2 \times 10^{-2} \times \|\widehat{u}_\tau\|_\infty$
- 800 adjoint iterations to achieve and cost about 15000 CPU-hours for the 600000 element meshes on the XSEDE cluster *Comet*

Z Wang et al., *Brain Multiphysics* (2021)

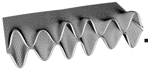

Conclusion

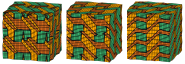

- VSI offers a powerful tool for identifying parsimonious models for a diverse set of physical systems.
- PDE Constrained Optimization can be used to fine-tune the sparse model.
- The dataset may influence the inferred model:
  - uncertainty in Bulk modulus in incompressible materials.
  - degeneracy in parameters in Ogden model.
- Smoothing noisy data improves convergence times in the inference procedure.
- Relevant Papers:

  Methodology(Z Wang et al., CMAME 2019; Z. Wang et al., Theoretical and Applied Mechanics Letters 2020; Z Wang et al., CMAME 2021; Z Wang et al., Computational Mechanics 2020; Z. Wang et al., arXiv:2104.14462v1 2021), **ACL**(J Estrada et al. Experimental Mechanics 2020; Z Wang et al., JMPS 2021), **Ogden Model**(D.P. Nikolov et al. , Philos. Trans. of Royal Society A 2022), **Brain Folding**(Z Wang et al., Brain Multiphysics 2021)